Extended Abstracts of the 17th Conference on Solid State Devices and Materials, Tokyo, 1985, pp. 421-424

**B-5-6**

# A New Technique of Exploiting Forward Nonlinear Reactance of P$^+$-N Junction

Jiang Guanhui

Nanjing Solid State Devices Research Institute

A new technique of exploiting the forward nonlinear reactance of P$^+$-N junction has been presented in this paper. A special model of impurity profile is offered which makes both variable amplitude and speed of the junction capacitance at forward bias greater than an abrupt junction model does. The new technique is used for fabricating GaAs varactors with M of 100-160 (at $f_{co}$=600-1000GHz, $\gamma_+$=0.2-0.27) being twice more than those manufactured by the abrupt P$^+$- N junction at same mobility. Those varactors are applied in investigating 4GHz un-cooled parametric amplifiers having the noise temperature of 32K. The experimental results coincide with the optimum computation of CAD.

## §1. Introduction

A carful analysis of the forward region of P$^+$- N junction demonstrates that the influence of the diffusion capacitance and forward current on devices is negligible at certain forward voltage for higher barrier semiconductor materials, such as GaAs(Table I); therefore, there exists possibility of exploiting the forward nonlinear reactance. A new model of impurity profile has been offered in this paper, which is used for fabricating GaAs varactors with higher changeable speed and greater variable amplitude of the P$^+$- N junction capacitance at forward bias than those of the abrupt junction, without decreasing cutoff frequency;hence the dynamic figure of merit M of P$^+$- N junction is much enhanced.

TABLE I Diffusion Capacitance and Forward Current of GaAs P$^+$- N Junction Via Forward Bias

| V(v) | 0.3 | 0.4 | 0.5 | 0.6 | 0.7 | 0.8 | 0.9 |
|---|---|---|---|---|---|---|---|
| C(pF) | $6.09\times10^{-9}$ | $2.8\times10^{-7}$ | $1.34\times10^{-5}$ | $6.24\times10^{-4}$ | $2.92\times10^{-2}$ | 1.37 | 63.9 |
| I(μA) | $1.58\times10^{-9}$ | $7.37\times10^{-8}$ | $3.45\times10^{-6}$ | $1.61\times10^{-4}$ | $7.55\times10^{-2}$ | $3.53\times10^{-1}$ | 16.5 |

## §2. A new technique model

1. A new model of impurity profile

The new impurity profile is shown in Fig 1, which is characterized by extending the space charge region at zero-bias to point $X_2$.

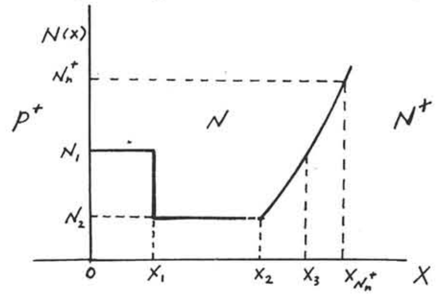


Fig. 1. The new model of impurity profile

There exists a jumped impurity profile for the space charge region of P$^+$- N junction at forward bias to enhance variable amplitude of the forward barrier capacitance, and hence the capacitance variation factor $\gamma$ is increased. Besides, because a larger variation of barrier capacitance is concentrated in a narrow region near zero bias, the slope of the C-V curve is also increased, which implies appreciable higher harmonic content. The region of $X_2$-$X_1$ is lower at concentration, but is covered by the space charge at zero bias. It is well known that the epitaxial layer covered by space charge at zero bias does not contribute series resistance. Meanwhile, the boundary of the space charge region correlated with minimum capacitance expands to point $X_3$ in the new model (See Fig. 1), thus enabling the transitional region, a burdensome in normal abrupt junction model, also to be partly used. Because of the above two reasons, the cutoff frequency at zero bias $f_{co}$ does not decrease with increasing $\gamma$, leading to an enhancement of M ( $=\gamma \cdot f_{co}$). The essence of this design is characterized by extending the space charge region at zero bias as far as to the point $X_2$.

2. C-V relation and the dynamic figure of merit M

By solving posson's equation the C-V relation of this technique can be described as [1]

$$V_D - V = \begin{cases} \dfrac{eN_1}{2\varepsilon\varepsilon_0}\delta_1^2 \\ \dfrac{eN_1}{2\varepsilon\varepsilon_0}X_N^2 + \dfrac{eN_2}{\varepsilon\varepsilon_0}X_N\delta_2 + \dfrac{eN_2}{2\varepsilon\varepsilon_0}\delta_2^2 \\ \dfrac{eN_1}{2\varepsilon\varepsilon_0}X_N^2 + \dfrac{eN_2}{\varepsilon\varepsilon_0}X_N X_M + \dfrac{eN_2}{2\varepsilon\varepsilon_0}\delta_2^2 + \dfrac{eN_2}{\varepsilon\varepsilon_0\beta^2} \\ \quad \cdot\left[e^{\beta\delta_3}(\beta\delta_3-1)+\beta(X_N+X_M)(e^{\beta\delta_3}-1)+1\right] \end{cases} \quad (1)$$

$$\delta = \begin{cases} \delta_1 \\ \delta_2 + X_N \\ \delta_3 + X_N + X_M \end{cases} \quad (2)$$

Where $N_2$ and $X_M$ in equation 1 and 2 are two important variables. Different capacitance Variation factors and cutoff frequen -cyies at zero bias respond to different combinations of $X_M$ and $N_2$, which decide the exploiting degree of forward nonlinear reactance. The numerical analyses of $X_M$ and $N_2$ by CAD are shown in Fig 2 and 3 [2].

Fig. 2 indicates that M of this model is a function of $N_2$ for each $N_1$ and M has an extreme value with the changeable of $N_2$. There is a corresponding $X_M$ for every $N_2$, which guarantees the space charge region at zero bias being extended to point $X_2$ (See Fig. 3).

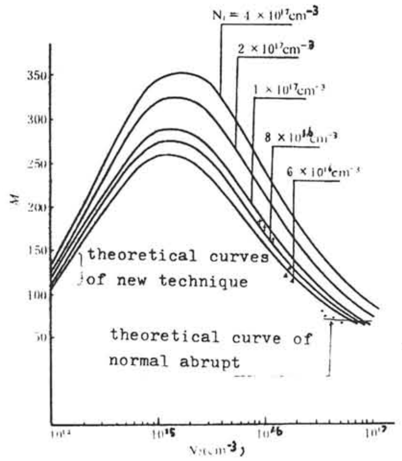


| | | |
|---|---|---|
| + $\frac{N_1}{N_2} \cong 10$ | M = 150 — 160 | $T_e$ = 32K |
| ▲ $\frac{N_1}{N_2} \cong 5$ | M = 90 — 120 | $T_e$ = 50K |
| • $\frac{N_1}{N_2} \cong 1$ | M = 60 — 80 | $T_e$ = 125K |

Fig. 2. The theoretical curves of $M \sim N_1$, $N_2$ and experimental results

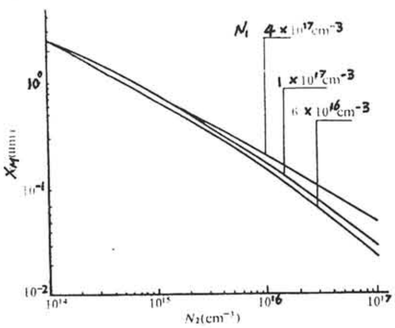


Fig. 3. The relation of $X_M \sim N_1, N_2$

§3. Experiments and Results

The epitaxial layer with the special profile is grown by VPE of a $Ga\text{-}AsCl_3\text{-}H_2$ system. The typical profile is shown in Fig. 4.

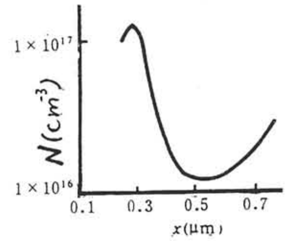


Fig. 4. The typical profile of an epitaxial layer

The $P^+$- N junction is formed by a planar diffusion technique, with the typical C-V curves of fabricated diodes being shown in Fig. 5. The relations of $M \sim N_1, N_2$ are shown in Fig. 2. From the definition of index n of $P^+$- N junction capacitance variation, n is the slope of curve $\lg C - \lg(V_D - V)$. In the new technique n of the forward region is expressed as

$$n = \frac{1}{2} \frac{\frac{N_1}{N_2} \frac{V_D - V}{V_D - V_{m1}}}{\left[ \left( \frac{V_D - V}{V_D - V_{m1}} - 1 \right) \frac{N_1}{N_2} + 1 \right]} \tag{3}$$

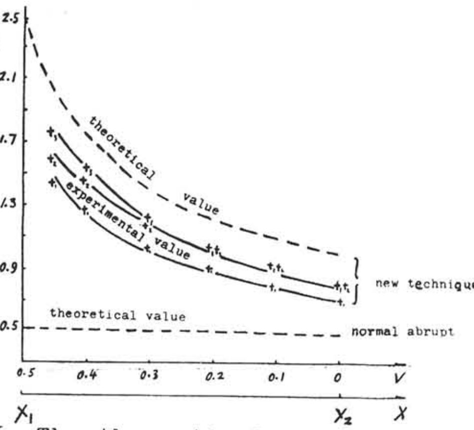


Fig. 6. The theoretical and experimental curves of $n \sim v$

From Fig. 5 and equation 3, theoretical curves of index n are obtained (See Fig. 6). When n is equal to 0.5, the devices have provided a secondary hamonic content. Therfore, it can be seen from Fig. 6 that the forward nonlinear reactance can provide appreciable higher harmonic content. This new technique is first used in fabricating GaAs varactor for 4GHz un-cooled parametric amplifiers with the noise temperature (Te) of 32K, and exhibits a superiority over the normal abrupt junction modle by which only 125K noise temperature can be reached (See Fig. 2)

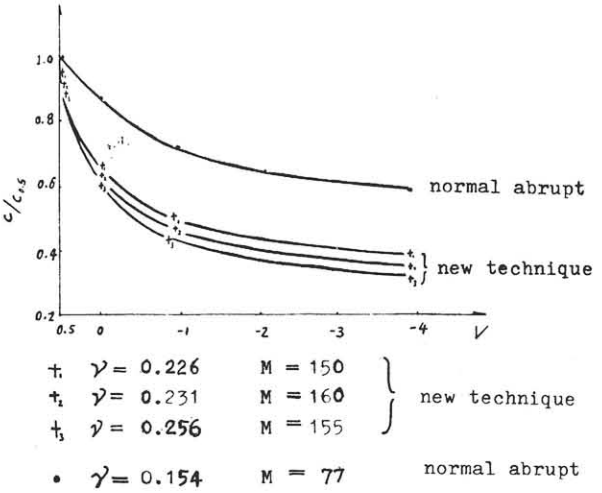


Fig. 5. The typical C-V curves

§4. Conclusion

A new technique of exploiting the forward nonlinear reactance for higher barrier semiconductor materials has been achieved. It can raise M and provide a appreciable higher harmonic content. It has been used in fabricating GaAs varactors for the paramatric amplifiers with significant improvement the noise temperature, and probably can also be employed for increasing the output power of a up-converter and offering an appreciable higher harmonic content of a harmonic generator.


Acknowledgement

The outhor wishes to thank Mr. Chen Qixiang, Luo Yunsheng, Chen Qidong, Shen Huimin and Sheng Wenwei for their supports.


References


1. Jiang Guanhui: CHINESE JOURNAL OF SEMICONDUCTOR 2 222 (1981)
2. Jiang Guanhui: RESEARCH & PROGRESS OF SSE NO 4 20 (1984)
3. Tian Mu: CHINESE JOURNAL OF SEMICONDUCTOR 1 220 (1980)
4. J.J.Harris and J.M.Woodcock: Electronic Letters 16 317 (1980)

Appendix

1. About Table I

$$C = A\ \frac{e^2 P_n^\circ}{kT} L_+\ e^{\frac{eV}{KT}}$$

$$I = Ae\left[n_p^\circ\left(\frac{D_-}{L_-}\right) + P_n^\circ\left(\frac{D_+}{L_+}\right)\right]\left(e^{\frac{eV}{KT}} - 1\right)$$
$$\cong A e P_n^\circ\left(\frac{D_+}{L_+}\right)\left(e^{\frac{eV}{KT}} - 1\right)$$

$$P_n^\circ = P_p^\circ e^{-\frac{eV}{KT}}$$

Take: $L_+ = 3.24\mu$ , $P_p^\circ = 1.05 \times 10^{20}\ cm^{-3}$ , $A = 300\mu^2$

2. Calculation of M

$$M = \gamma \cdot f_{co}$$

$$f_{co} = \frac{1}{2\pi R_s C_{j0}}$$

$$R_s = R_{Au} + R_N + R_L + R_B + R_P$$

$$R_{Au} = \frac{\rho_{Au}\, \ell_{Au}}{2\pi}\ \frac{1}{d_{Au}(2Y_{Au} - d_{Au})}$$

$$R_L = \frac{X_L}{e\mu_n \pi R^2 N_2 \ln(N_n^+/N_2)}$$

$$R_B = \frac{\rho_B}{2\pi R}\tan^{-1}\frac{Y_S}{R} + \frac{\rho_B}{2\pi d_N}\ln\frac{Y_S}{R} + \frac{\rho_B(t-d_N)}{\pi d_N(2Y_S - d_N)}$$

$$R_P = \frac{1}{\pi R^2}\rho_P$$

$R_N =$ measured Value

$$C_{j0}^{(3)} = \frac{\varepsilon\,\varepsilon_o}{\delta(V_o)}\pi R^2\left\{1 + \frac{\pi}{R}\left[X_j + \delta(V_o)\right]\right\} + C_{ad}$$

$$\gamma = \frac{1}{2}\ \frac{\Gamma - 1}{\Gamma + 1}\ ^{(4)}$$

$$\Gamma = \frac{\Gamma^{**} E_d + A_d}{1 + A_d}$$

$$\Gamma^{**} = \frac{\delta(V_{min})}{\delta(V_{max})}$$

$$A_d = \frac{C_{ad}}{C^*_{min}}$$

$$C^*_{min} = \frac{\varepsilon\ \varepsilon_o}{\delta(V_{min})}\pi R^2\left\{1 + \frac{\pi}{R}\left[X_j + \delta(V_{min})\right]\right\}$$

$$E_d = \frac{1 + \frac{\pi}{R}\left[X_j + \delta(V_{max})\right]}{1 + \frac{\pi}{R}\left[X_j + \delta(V_{min})\right]}$$

Take:

$\rho_{Au} = 2.21 \times 10^{-6}\ \Omega cm$
$\rho_B = 0.78 \times 10^{-3}\ \Omega cm$
$\rho_P = 1.0 \times 10^{-6}\ \Omega cm$
$\mu_n = 3500\ cm^2/V\cdot S$
$\ell_{Au} = 0.15\ mm$
$Y_{Au} = 5\ \mu$
$X_L = 0.15\ \mu$
$t = 90\ \mu$
$Y_S = 120\ \mu$
$X_j = 0.3\ \mu$
$V_{m1} = 0.5\ V$
$V_{m2} = 0\ V$
$V_{min} = -4V$
$V_{max} = 0.5V$

$V_D = 1.2\ V$
$V_o = 0\ V$
$N_n^+ = 4 \times 10^{18}\ cm^{-3}$
$R_N = 0.1\ \Omega$
$\varepsilon\varepsilon_o = 11.1 \times 8.85 \times 10^{-14}\ F/cm$
$C_{ad} = 0.01\ PF$

The deepth of skin effect at 60GHz

$d_{Au} = 0.265\ \mu$ (Au)
$d_N = 4.97\ \mu$ (GaAS)